

# Active Triangulation Scanner Development Focusing on the Accuracy of the Detection

## **Tibor Kovács**

Department of Automation  
Budapest University of Technology and Economics,  
H-1111 Budapest, Goldmann Gy. tér 3.  
HUNGARY  
E-mail: kovacs.tibor@aut.bme.hu

*A 3D active triangulation scanner is under development at the Department. The project is focusing on the cost-effective realisation, controlled accuracy and easy practical use. The main difficulty is the distortion caused by the noise in the frame buffer. In this publication a noise model will be defined, the method of the noise model validity examination will be drafted. With that a novel line following algorithm will be defined, that is able to take into account the effect of the noise and can estimate the accuracy based on statistical consideration. Final part of the paper presents results of the research and define future directions, shows a possible industrial application.*

*Keywords: 3D scanner, line following, noise model*

## **1. The Target of the Project**

The target of this development is to create a 3D scanner to produce 3D models for CAD/Visualisation systems, like 3D Studio Max [5][13]. These models can be used for advertisement, game development or reverse engineering. In the market a lot of scanner devices can be found, but these devices do not focus on the information about accuracy [6]. Naturally some commitment to the general accuracy of the device can be found in the user's manual, but generally there is no information on the accuracy of the actual scan. So the development highlights the following criteria:

- Numerical information about the accuracy of the actual scan based on some environmental parameters (noise, configuration parameters)
- Development of a cheap device: the accurate model generation is reached via algorithmic solutions instead of expensive hardware elements

## 2. Experimental Device Layout

The experimental device is an active triangulation scanner based on a vertically structured light source [1]. This device is built up as an experimental device to study the nature and the effect of the noise in the frame buffer and to elaborate the line following algorithm.

Main components of the scanner is the rotating table, the light source and the imaging device (camera) [2]. The layout is presented in the *figure 1*.

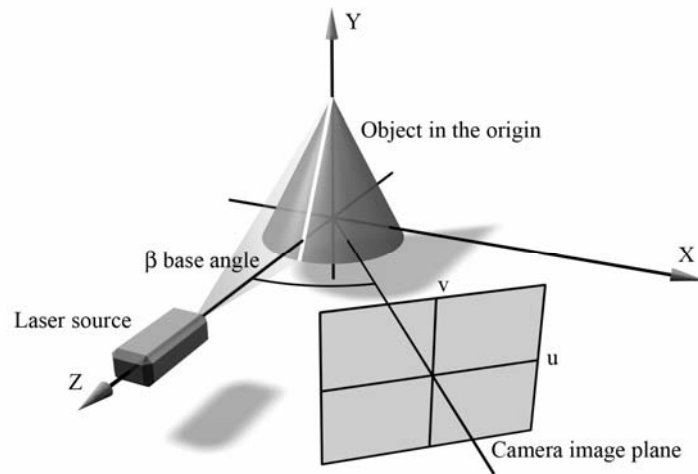


*Figure 1. Layout of the experimental scanner system*

### 2.1. Object Table

The object table can be rotating table to scan cylindrical objects or it can be sliding table to scan bas relief-like objects. The actual cross section parameter (rotating angle of shift of the sliding table) is set by step motor.

### 2.2. Light Source

The light source is a 5 mW He-Ne laser. A cylindrical lens is used for shaping a vertical line projected to the object on the table. It is important that the intensity profile of the laser beam is Gaussian [14].

### **2.3. The Imager Device**

Formerly a 512x512 pixel resolution Visionetics frame buffer and a JVC TK-870E camera head were used. Now development is focused on to the progressive scan programmable digital cameras. First the most important topic is to choose the technology: which is the lowest noise camera, which technology is the best (CCD or CMOS).

### **3. Noise Model**

It is assumed that the image of the imager subsystem is loaded by noise characterized as follows: independent, Gaussian distribution zero mean additive noise (random variable), with variance  $\sigma_N$  [11]. In this model the noise is independent from the intensity and from the frame buffer position as well. This assumption proved to be a good approach in the course of our experiments, however further research is in progress to confirm validity and expose limits of this model [3].

The verification of this assumption is under processing. A homogeneous white area will be defined and homogeneous lighting will be installed. A statistically relevant amount of pictures will be captured about this surface under different illumination circumstances (for instance 5 levels of intensities covering the whole gray domain of the imager system from almost black to almost white). Based on this sample the behavior of the noise can be get known.

## **4. Line Following Algorithm**

### **4.1. Initial Point Finding**

The first step is to find a potential initial point for the line following. Therefore  $u$ -directed scanlines are examined. The line tracking algorithm is designed to generate a point sequence with real  $(u,v)$  rather than integer coordinates, because it is necessary to improve the accuracy of the line extraction. The starting point of the line tracking should be found with real coordinates as well, instead of inaccurate integer coordinates [12]. The starting point can be determined in the defined image field as the symmetry point of a Gaussian curve fitted to intensities measured along a scan line. The square error distance is used as a fault scale of curve regression [4].

Let intensities of the sample be  $p_i$ ,  $i=1, 2, \dots, n$ . It is a continuous set of intensities above a certain threshold, including the potential initial point. This threshold can

be set experimentally, for it depends on the noise level and it must be high enough to define the environment of a real starting point. The curve to be fitted is given by

$$p_i = f(u_i) = A \cdot \exp \frac{-(u_i - m)^2}{B} \quad (1)$$

where  $m$  is the coordinate  $u$  of the starting point.

By setting normal equations the starting point of the line tracking  $m$  can be determined:

$$m = \frac{\sum_{i=1}^n (u_i - \bar{u}) \ln p_i}{2 \sum_{i=1}^n (u_i - \bar{u})^2} \cdot \frac{\left( \sum_{i=1}^n (u_i - \bar{u})^2 \right)^2 - n \sum_{i=1}^n (u_i - \bar{u})^4}{n \sum_{i=1}^n (u_i - \bar{u})^2 \ln p_i - \sum_{i=1}^n \ln p_i \cdot \sum_{i=1}^n (u_i - \bar{u})^2} + \bar{u} \quad (2)$$

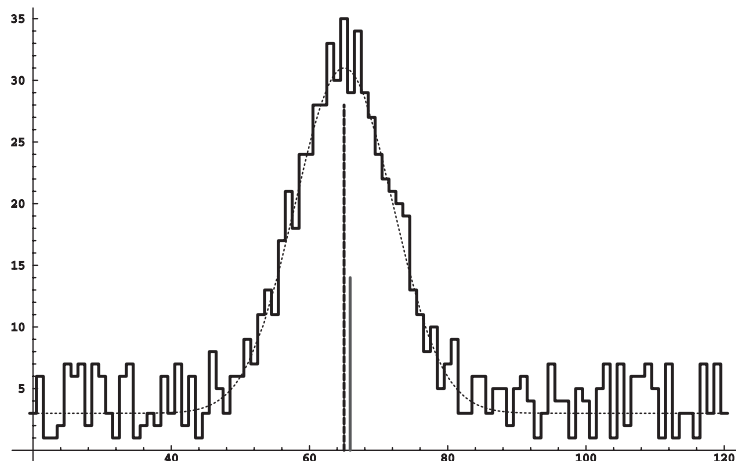


Figure 2. It demonstrates the result of the method in synthetic experimental environment. An noiseless gaussian intensity profile was generated with maximum position  $u=65$ . This profile was corrupted with synthetic noise defined in section 3. The algorithm defined by equation 2 has found the maximum point at  $u=65.88$ . So the difference between the ideal, unnoisy maximum position and the output of the algorithm is 0.88 pixel, because of the random noise.

## 4.2. Recursive Step Forward

In the camera coordinate system  $(u,v)$  a  $v$ -directed and a  $(-v)$ -directed line following process are started from the initial point found by the algorithm defined by equation 2 [9][10]. Later the two parts of the profile are linked into a continuous curve. Tasks to be executed in the two directions are similar, apart from the slight differences due to the different direction. The noise of the frame

buffer disturbs the calculation of the next direction in this recursive process, so there will be a slight discrepancy between the ideal line and the extracted curve. An averaging filtering is applied to reduce this discrepancy. The filter process can be calibrated by a scalar parameter, the scale of the filter. It is the radius of the averaging kernel window (the window is a  $2s+1$  sized square). The accuracy of the line tracking can be characterized in the following way. The accuracy can be increased by increasing the parameter  $s$ , but it should not be too high, because a high  $s$  value makes the line too smooth, in the meantime reducing the sensitivity of the algorithm.

Let  $D$  be the direction of the current step.  $D$  is an angle, 0 in the positive  $v$  direction, which is increasing clockwise to  $\pi$  and decreasing counter-clockwise to  $-\pi$ .

Let  $I_{u,v}$  be the intensity function or image matrix in the frame buffer.  $I_{u,v}$  is composed of the noiseless  $F_{u,v}$  image function and the  $N_{u,v}$  noise defined above:

$$I_{u,v} = F_{u,v} + N_{u,v} \quad (3)$$

To simplify the indexing in the line tracking window a filter window coordinate system is defined for the  $2s+1$  sized window. Coordinates are denoted as  $i$  and  $j$ ,  $i=-s, \dots, 0, \dots, s$ ,  $j=-s, \dots, 0, \dots, s$ . Let  $\varphi_{i,j}$  be an angle matrix:

$$\varphi_{i,j} = \arctan \frac{i}{j} \quad (4)$$

If  $j=0$ ,  $\varphi_{i,j} = \text{sgn}(i)\pi/2$  (if  $x>0$ ,  $\text{sgn}(x)=1$ , if  $x=0$ ,  $\text{sgn}(x)=0$ , if  $x<0$  then  $\text{sgn}(x)=-1$ ). So the element  $\varphi_{a,b}$  contains the angle of the vector  $((0,0);(a,b))$ .

If the whole area of the  $2s+1$  sized filter window is used above the  $I_{u,v}$  intensity matrix, a slight anisotropy can be detected. The distance of the farthest pixels (for example  $(i=-s;j=s)$  or  $(i=s;j=s)$ ) from the filter kernel center  $(i=0;j=0)$  at the direction  $\pm\pi/4$  is  $\sqrt{2}$  times higher than pixels  $(i=0;j=s)$ ,  $(i=-s;j=0)$  or  $(i=s;j=0)$  at the direction 0 or  $\pm\pi/2$ . A special kind of masking is applied to limit the considered  $I_{u,v}$  pixels.

Let  $A'_{i,j}$  be the circular limit mask matrix.  $A'_{i,j}=1$ , if the whole surface of the  $(i,j)$  pixel is in the circle  $i^2+j^2-s^2=0$ . For the four corners of the  $(i,j)$  pixel:

$$\begin{aligned} (i-0.5)^2 + (j-0.5)^2 - s^2 &\leq 0 \\ (i+0.5)^2 + (j-0.5)^2 - s^2 &\leq 0 \\ (i-0.5)^2 + (j+0.5)^2 - s^2 &\leq 0 \\ (i+0.5)^2 + (j+0.5)^2 - s^2 &\leq 0 \end{aligned} \quad (5)$$

If all inequalities in *formula 5* meet a ‘greater then or equal’ relation then  $A'_{i,j}=0$ . Otherwise  $A'_{i,j}$  is the area of the intersection of the pixel  $(i,j)$  surface and the circle defined above. *Figure 3a* presents a graphic description of the  $A'$  matrix.

The  $D$  direction of the extracted line is considered to vary continuously. Half of the filter window can be considered at the calculation of the direction, because the other half marks the opposite direction. Let  $D'$  be the direction of the previous iteration of the line tracking algorithm. Let the directional mask  $A''_{i,j}$  be defined as  $A''_{i,j}=1$  if

$$\begin{aligned} \text{ctg}(D') \cdot (i - 0.5) - (j - 0.5) &\leq 0 \\ \text{ctg}(D') \cdot (i + 0.5) - (j - 0.5) &\leq 0 \\ \text{ctg}(D') \cdot (i - 0.5) - (j + 0.5) &\leq 0 \\ \text{ctg}(D') \cdot (i + 0.5) - (j + 0.5) &\leq 0 \end{aligned} \quad (6)$$

for the four corners of the  $(i,j)$  pixel. If all inequalities in *formula 6* meet a ‘greater then or equal’ relation then  $A''_{i,j}=0$ . Otherwise  $A''_{i,j}$  is the area of the intersection of the pixel  $(i,j)$  surface and the half plane defined in *formula 6*. *Figure 3b* presents a graphic description of the  $A''$  matrix. A more detailed approach is described in [8].

Let the  $A_{i,j}$  mask matrix be defined as

$$A_{i,j} = A'_{i,j} \cdot A''_{i,j} \quad (7)$$

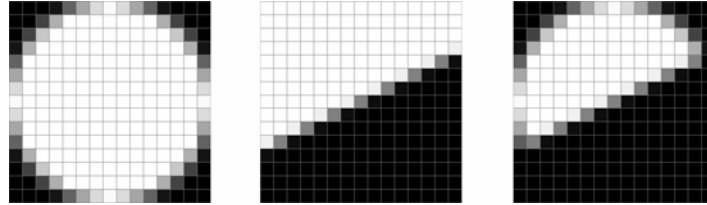


*Figure 3. A graphic representation of the  $A$  matrix is shown. White pixels denote values of 1, black pixels have value of 0, and inbetween the grey-shade pixels have values between 0 and 1. *Figure 3a* shows the circular limit denoted  $A'$ , *figure 3b* describes directional limit denoted  $A''$  and *figure 3c* is the  $A$  matrix derived as the cell by cell logical AND of them.*

The current step direction  $D$  of the line tracking can be calculated as a weighted average of the elements of  $\varphi$  angle matrix with the proper part of the whole  $I$  intensity matrix masked with the  $A$  mask matrix:

$$D = \frac{\sum_{i=-s}^s \sum_{j=-s}^s I_{u+i,v+j} \cdot A_{i,j} \cdot \varphi_{i,j}}{\sum_{i=-s}^s \sum_{j=-s}^s I_{u+i,v+j} \cdot A_{i,j}} \quad (8)$$

## 5. The Precision of the Angular Computation

Let us analyse the relation between the scale of the filter window and the accuracy of the direction of the next step. The filter window contains  $w=(2s+1)^2$  pixels taken into consideration in the algorithm. Each pixel intensity is the sum of the deterministic image sign  $F_{u,v}$  and a random variable  $N(0, \sigma_N)_{u,v}$  representing the noise defined previously.

$$D = \frac{\sum_{i=-s}^s \sum_{j=-s}^s F_{u+i,v+j} \cdot A_{i,j} \cdot \varphi_{i,j} + \sum_{i=-s}^s \sum_{j=-s}^s N_{u+i,v+j} \cdot A_{i,j} \cdot \varphi_{i,j}}{\sum_{i=-s}^s \sum_{j=-s}^s F_{u+i,v+j} \cdot A_{i,j} + \sum_{i=-s}^s \sum_{j=-s}^s N_{u+i,v+j} \cdot A_{i,j}} \quad (9)$$

*Formula 9* transforms random variables  $N_{u,v}$  to a random variable  $D$ . It can be shown that there is a relation between a given discrepancy  $d$  of the step direction, the window size  $2s+1$ , and the probability that the step direction will deviate from the mean more than  $d$ .

The essential step of the deduction is the application of the Chebyshev-inequality [3]. It is necessary to determine the variance of  $D$  presented in *formula 9*. The task is to calculate the variance of the quotient of the independent random variables. An approximation is applied. Let us take the first two elements of the Taylor series of  $D(N_1, \dots, N_w)$  close to  $\theta$  based on the formula

$$D(N_1, \dots, N_w) \cong D(0, \dots, 0) + \sum_{k=1}^w \frac{\partial D}{\partial N_k} \Big|_{0, \dots, 0} N_k \quad (10)$$

The partial derivative of  $D$ :

$$\frac{\partial D}{\partial N_k} = \frac{\left( \sum_{i,j} FA + \sum_{i,j} NA \right) \cdot A_k \varphi_k - \left( \sum_{i,j} FA \varphi + \sum_{i,j} NA \varphi \right) \cdot A_k}{\left( \sum_{i,j} FA + \sum_{i,j} NA \right)^2} \quad (11)$$

$$D \cong T(D)_1 = \frac{\sum_{i,j} FA \varphi}{\sum_{i,j} FA} + \sum_{k=1}^w \left[ \frac{\sum_{i,j} (FA) A_k \varphi_k - \sum_{i,j} (FA \varphi) A_k}{\left( \sum_{i,j} FA \right)^2} N_k \right] \quad (12)$$

The variance can be expressed as

$$\sigma_D^2 \cong \sigma_T^2 = \sigma_N^2 \cdot \sum_{k=1}^w \left[ \frac{\sum_{i,j} (FA) A_k \varphi_k - \sum_{i,j} (FA \varphi) A_k}{\left( \sum_{i,j} FA \right)^2} \right]^2 \quad (13)$$

The mean of  $D$  is  $E(D)$ , the ideal, error-free direction, the variance is  $\sigma_D$ ,  $d$  is the given angle-error,  $P$  is the probability of the deviation of the direction larger than  $d$ :

$$P(|D - E(D)| \geq d) \leq \frac{\sigma_D^2}{d^2} \quad (14)$$

The variance depends on the ideal image function, so practically a typical  $F$  pattern can be substituted into this formula, and a table can be created. The  $s$  runs from 1 to a practical maximum (for instance 10) and under the supposed  $F$  pattern  $\sigma_D^2$  can be calculated. As a result following questions can be answered in connection with  $s$ ,  $d$ , and  $P$ . The line mapped in the frame buffer can be extracted with preliminary calculated statistical accuracy. The adequate table with actual noise distribution and  $s$  value can be created in a given environment, so the accuracy of the resulted model can be controlled. For instance using the Chebyshev formula under  $w=10$  line width,  $\sigma_N=0.3$  noise and applying  $s=3$  line following, the probability of one degree deviance between the ideal and the real directions is less than or equal to 0.2231. Under similar conditions applying  $s=7$  method the mentioned probability can be decreased to near 5%.

## 6. The Controlled Scanning Process

The following methodology enables the effective operation of the scanner system. This section describes how the accuracy of the model can be influenced and analysed at different points of the algorithm. Procedures are drafted for the calculation of some system parameters as well.

### 6.1. Measurement and Setting of System Parameters

Current lighting profile of the target object must be known to be able to set up the sensitivity of the imaging system. It depends on the colour of the object, other optical parameters of the surface (for instance the reflectance), the environmental lighting, etc. If the sensitivity is run from a minimum value, the optimal value is reached, when the profile peak has the maximum intensity value, but the profile is not saturated, it does not have a maximum value plateau.

It is necessary to calculate the width of the profile at half-intensity level, characterizing the object, the environment and the lighting. Based on results of section 4.1.  $B$  can be calculated:

$$B = -\frac{1}{\beta_2} \quad (15)$$



The width of the profile at half-intensity is

$$c = \sqrt{-B \cdot \ln 0.5} \quad (16)$$

For the statistical prediction of the accuracy it is necessary to measure the parameters of the noise. If a homogeneously lit surface is taken supposing an unnoisy frame buffer content, a certain grey value will be resulted at every pixel. This image is corrupted by noise. Take a statistically significant sample of this image, for instance pixels of a scan line. The variance can be calculated based on the following expression on the variance  $\sigma^2$  of that noise:

$$\sigma^2 = \frac{\sum_{i=1}^n e_i^2}{n-1} \quad (17)$$

where  $n$  is the number of elements in the sample,  $e_i$  is the difference between the  $y_i$  intensity and the average of the set.

The *line threshold* is the minimum intensity value, that is considered as a line to determine the initial point rather than a background point. Let its value be significantly higher than the average intensity of dark areas (for instance half of the maximum intensity value). The *noise threshold* is the minimum intensity value, that should be considered to a point of a line in the line tracking algorithm. Noise threshold has to be set to at least  $I_0 + \sigma$ , where  $I_0$  is the average intensity of dark areas. In this way the tracked line can be separated from the dark background, and the longest line can be extracted.

Finally Chebyshev-tables have to be calculated (based on section 5.). The line tracker works in the camera coordinate system, so the error is measured in this system as well. It can be transformed into the world coordinate system. The filter window size  $2s+1$  can be set in a way, that the error of the resulted profile and the assigned probability  $P$  meets the user-defined conditions.

Setting system parameters described in this section model creation can be started. Optical features of the surface, some kind of geometrical distortions, and the noise of the imaging system are taken into consideration in initial system parameters.

## Conclusions

The active triangulation scanner described before is a low cost device that can handle the inaccuracy caused by the noise in the frame buffer. This noise is modelled with independent Gaussian noise. The validity of this model is partially proven, and one of the most important tasks is to exactly define the usability of this model. An other main development direction is to enhance the algorithm to take into consideration the intensity profile of the laser beam.

The output of the system is not only a vertex cloud. The builder modul can assemble the model as a polygon mesh, even later a NURBS surface [4]. The builder module is designed to create morphable targets about totally different objects.

A strong future direction of the development is to apply these results in mechanical reengineering [7]. A cooperation is built with an industrial partner up, where a SCANTECH scanner is applied for 3-5 axis CNC and CMM machinery. The target of the cooperation is to enhance the precision of scanning [6].

Finally two examples are presented created before with this scanner.

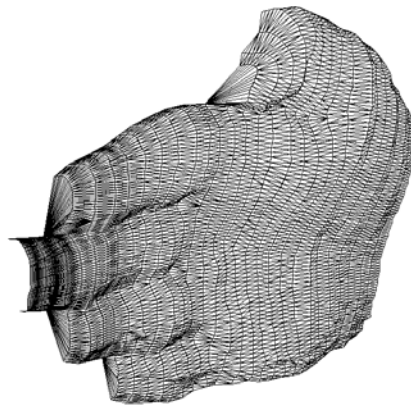


*Figure 4. Human hand scanned with translation table*

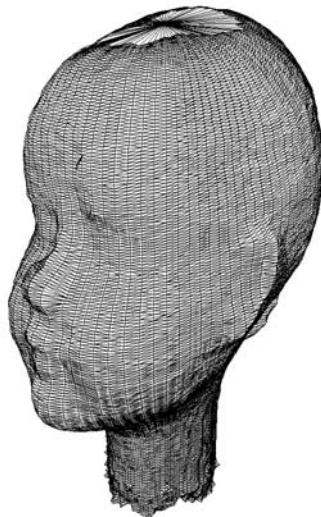


*Figure 5. Plaster head scanned with rotating table*

## References

- [1]. Yoshiaki Shirai: Three-Dimensional Computer Vision, Springer Verlag, 1987.
- [2]. Jorge L.C. Sanz: Advances in Machine Vision, Springer Verlag, 1989.
- [3]. Jan Ludvik, Radimir Vrba: Image Processing Noise Removal using a Cellular Neural Network, 2002 WSEAS Int.Conf. on Information Security, Hardware/Software Codesign, E-Commerce and Computer Networks, Copacabana, Rio de Janeiro, Brazil, 2002.
- [4]. I. Vakalis (Italy): Digital Topology: A survey of 3D object representation and its configuration space, 3th WSEAS CSCC (WSEAS International Multiconference on Circuits, Systems, Communications and Computers), Athens, Greece, 1999.
- [5]. Marc Rioux: Applications of Digital 3D Imaging, Canadian Conference on Electrical and Computer Engineering, 1990.09.03-06., pp. 37.3.1-37.3.10
- [6]. Terry T. Wohlers: 3D Digitizers, Computer Graphics World, 1992.07., pp. 73-77
- [7]. Francois Blais, Marc Rioux, Jacques Domey: Optical Range Image Acquisition for the Navigation of a Mobile Robot, IEEE International Conference on Robotics and Automation, 1991.04.09-11, pp. 2574-2580
- [8]. Alan Watt, Mark Watt: Advanced Animation and Rendering Techniques, Theory and Practice, Addison-Wesley, 1992.
- [9]. Kae-Jy Chou, Brian G. Schunck: Nonparametric Algorithm for Edge Localization, IEEE Computer Vision and Pattern Recognition, 1993., pp. 795-796
- [10]. Chris Davatzikos, Jerry L. Prince: Adaptive Active Contour Algorithms for Extracting and Mapping Thick Curves, IEEE Computer Vision and Pattern Recognition, 1993., pp. 524-529
- [11]. Michael Margaliot, Craig Gotsman: Piecewise-Linear Surface Approximation from Noisy Scattered Samples, IEEE Visualisation Conference, 1994., pp. 61-68
- [12]. Wolfgang Beil: Line Detection in Discrete Scale-Space, 1st IEEE International Conference on Image Processing Vol. 1., 1994., pp. 915-918
- [13]. Crispin Littlehales, Marc Rioux: White Light Magic, IRIS universe, the magazine of visual computing, number eighteen, Siliicon Graphics Inc., 1992., pp. 24-27
- [14]. John E. Harry: Industrial Lasers and Applications (Ipari lézerek és alkalmazásuk, in Hungarian), Műszaki Könyvkiadó, 1979.